Robust Super Twisting Based Sliding Mode Control for a 2-DOF Nonlinear Helicopter Model

Jasmin Velagic and Salko Vladavic

Abstract— **This paper presents a robust control strategy, namely Sliding Mode Control (SMC), to control a two-degree-of-freedom (2DOF) helicopter model. This model is an inherently unstable, nonlinear, and multivariable system with coupling effects between two axes. Due to the mentioned characteristics, helicopter control remains a challenging problem, especially in the presence of external disturbances, parameter perturbation and model uncertainties. In order to overcome some of these difficulties, we developed a second order sliding mode controller based on the super-twisting algorithm (STSMC). It represents a modification of the standard SMC with the aim of improving its control capabilities. The effectiveness and robustness of the used STSMC were verified through simulations and experiments. The results obtained were compared with the same achieved by a previously developed PID and adaptive controllers. The STSMC significantly outperforms the PID controller and additionally improves the efficiency of the used adaptive controller in terms of stability of the system, tracking error, and overall control performance in the presence of system uncertainties and coupling effects between two axes, the azimuth and elevation.**

I. INTRODUCTION

Nonlinear systems play a vital role in modern control engineering, since all plants in practice are mainly nonlinear in nature [1]. The study of nonlinear systems is attracting increasing attention from researchers to explore the use of nonlinear control methods as a way of coping various issues encountered when using linear control of nonlinear processes. [2], [3]. One such nonlinear, inherently unstable, dynamic system is a helicopter model with two degrees of freedom (2DOF), which is the subject of this paper. In the last two decades, helicopters have received increased attention because they offer a wide range of various applications, including the transport of people and cargo, search and rescue missions, military and police operations, medical transportation, firefighting operations, aerial observations, and air pollution monitoring, among others [2]. These applications are possible because of the helicopter's ability to take off and land vertically, to hover, and to fly forward, backward, and laterally.

Regarding a flight control of the helicopter system, conventional strategies involve linearizing the dynamics of the nonlinear helicopter model around a set of preselected equilibrium points. These control techniques are mainly based on SISO (sultiple-input-single-output) approaches with PID control laws. However, this requires multi-loop controllers, which make their design inflexible and difficult to tune controller parameters. Afterwards, in our paper we consider a multi-input-multiple-output (MIMO) nonlinear helicopter model which is used as a plant in modern control theory [4]. It includes the use of advanced controllers, such as gain scheduling [5], linear quadratic regulator (LQR) control [6], loopshaping-based controller [7], model predictive control (MPC) [8], robust sliding mode control [9], nonlinear h_∞ control [10], various types of adaptive-fuzzy [11], [12] control, backstepping [13], neural network [14], etc.

The controlled system used in our paper is HUMUSOFT's CE 150 helicopter model. It is a good case study of nonlinear system control, suitable for testing any control techniques aimed at supervision of nonlinear behavior. This MIMO model consists of three potential inputs (voltages), one input for each of the two DC motors responsible for driving the propellers, and one for manipulating the center of gravity. Motor input voltages have a linear relation with the torques generated. The output of the helicopter model represents the azimuth and elevation angles, which are measured by incremental encoders. The helicopter model shows strong cross-coupling effects between the elevation and azimuth dynamics. This means that the operation of one motor affects the performance of another. Among other factors, cross-coupling increases the difficulty of proper control design. The system is fixed on a base and contained in a cage in order to minimize the risk of damage to both the working environment and the system. Direct communication with the physical model of the CE 150 helicopter is established using Real-Time Toolbox, which is an integral part of Matlab/Simulink environment. Information about the system was extracted from [15], which is referred to for more information.

In this paper, the STSMC is developed with the aim of simultaneously tracking the azimuth and elevation position references of the nonlinear multivariable helicopter model. This controller deals with system uncertainties caused by cross-coupling action between the azimuth and elevation axes. In addition, the proposed STSMC can cope effectively with the nonlinear characteristics of the used 2DOF helicopter model. In order to overcome the above difficulty and improve the helicopter tracking performance, some modifications have been made to the SMC.

The paper is structured as follows: Section II describes and explains the used 2DOF multivariable and nonlinear helicopter model. In Section III the second-order sliding mode controller (STSMC) is developed with the aim of coping with high nonlinearities and cross-coupling effects of the helicopter. The evaluation of the control performance of

Jasmin Velagic and Salko Vladavic are with Faculty of Electrical Engineering, University of Sarajevo, 71000 Sarajevo, Bosnia and Herzegovina (jvelagic, svladavic1)@etf.unsa.ba

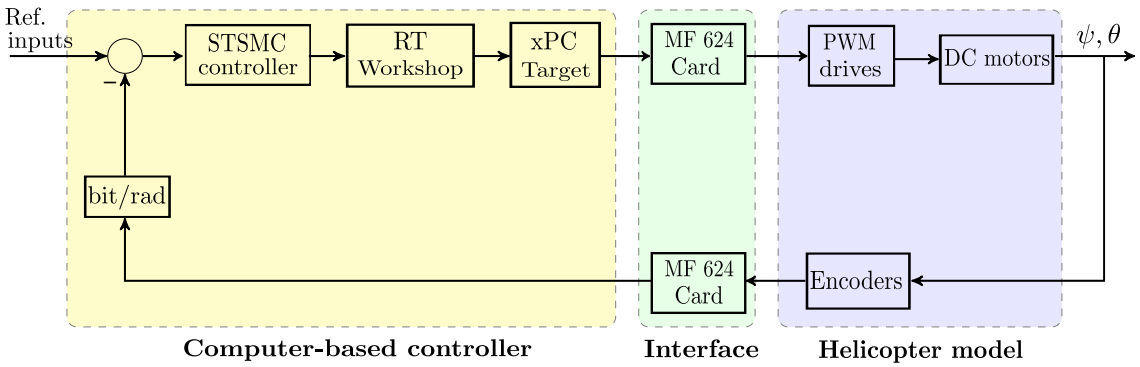

Fig. 1. Proposed real-time control scheme for helicopter model

the proposed STSMC compared to the previous designed PID controllers is done through both simulations and experiments in Sections IV and V. Section VI summarizes our findings and gives a brief exposition of future research directions.

II. CONTROL SYSTEM DESCRIPTION

The proposed real-time control system for the Humusoft CE150 2DOF helicopter model is shown in Fig. 1. The overall system includes: i) PC based STSMC controllers, ii) interface module and iii) real-helicopter system. More details on the control interface used can be found in [14]. The helicopter is modeled for purposes of controller synthesis and performance tracking validation. The used helicopter is a rigid body with two DC motors driving the main and side rotors, power amplifiers, and encoders as sensors (Fig. 2).

The helicopter model used has two degrees of freedom: elevation angle ψ representing rotation around the horizontal axis and azimuth angle θ representing rotation around the vertical axis. The axes of the main and side propellers are orthogonal. The helicopter model is a MIMO system with two input signals (voltage of the main motor u_1 and voltage of the side motor u_2 with operation ranges $[0, 0.8]$ and $[0, 0.3]$, respectively) and two output signals (elevation and azimuth with operation ranges $[-45, 45]$ degree and $[-135, 135]$ degree, respectively).

The equations of helicopter motion in the vertical and horizontal planes are derived using the Euler-Lagrange equations

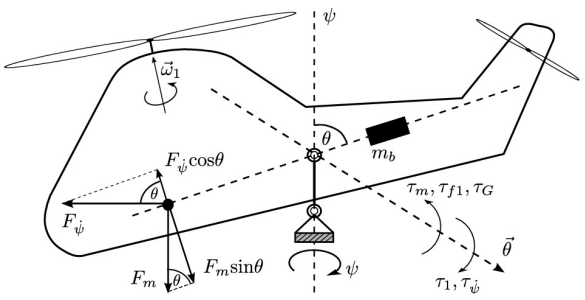

Fig. 2. Simplified helicopter model with two inputs and two outputs

given by elevation dynamics:

$$a_\psi \ddot{\psi} = \tau_1 + \tau_{\dot\theta} - \tau_{f_1} - \tau_m + \tau_G, \tag{1}$$

$$\tau_m = mgl \sin\psi, \tag{2}$$

$$\tau_{\dot\theta} = ml\dot\theta^2 \sin\psi \cos\psi, \tag{3}$$

$$\tau_{f_1} = C_\psi \operatorname{sign}\dot\psi + B_\psi \dot\psi, \tag{4}$$

$$\tau_G = k_G \dot\theta \omega_1 \cos\psi, \text{ for } \dot\theta \ll \omega_1, \tag{5}$$

and azimuth dynamics:

$$a_\theta \ddot{\theta} = \tau_2 - \tau_{f_2} - \tau_r, \tag{6}$$

$$\tau_{f_2} = C_\theta \operatorname{sign}\dot\theta + B_\theta \dot\theta, \tag{7}$$

$$a_\theta = a_\psi \sin\psi. \tag{8}$$

where: a_ψ is moment of inertia around horizontal axis, τ_1 is moment produced by the main motor propeller, $\tau_{\dot\theta}$ is centrifugal torque, τ_{f_1} is Coulomb and viscous friction torques, τ_m is gravitation torque, τ_G is gyroscopic torque, m is mass of the helicopter body, g is gravitational acceleration, l is distance from z axis to main motor axis, ω_1 is angular velocity of the main propeller, k_G is gyroscopic coefficient, B_ψ is viscous friction coefficient, C_ψ is Coulomb friction coefficient, a_θ is moment of inertia around vertical axis, τ_2 is moment produced by the side motor propeller, τ_{f_2} is Coulomb and viscous friction torques, τ_r is reaction torque of the main motor, ω_2 is angular velocity of the side propeller, B_θ is viscous friction coefficient, C_θ Coulomb friction coefficient.

In addition, the dynamics of the main and tail motor model can be described as a second-order transfer function[16]:

$$\frac{\omega_i(s)}{u_i(s)} = \frac{1}{(T_i s + 1)^2}, \tag{9}$$

where $\omega_i(s)$ and $u_i(s)$ are Laplace transforms of $\omega_i(t)$ and $u_i(t)$ respectively, while T_i is the time constant of the main motor ($i = 1$) and the tail motor ($i = 2$).

Detailed description of the helicopter used and the identification of its individual parameters can be found in [17]. It was necessary to identify 14 unknown parameters. The identification procedure was performed experimentally, but there is some uncertainty about the accuracy of all parameters. Also, it is necessary to take into account an existing

strong cross-coupling and significant nonlinearities in the model itself. Since the mathematical model of the system has some uncertain parameters, it is needed to use some variant of the robust control. Our paper focuses on one of the robust control strategies, more precisely the sliding mode control.

III. SLIDING MODE CONTROL

One of the promising techniques for designing robust control laws is the sliding-mode control. It represents a nonlinear control approach which provides robustness to parameter variations, reduced order of sliding-mode dynamics, and finite-time convergence to zero for sliding-mode variables [18]. The main idea of SMC is the design of a surface in the state space of the system that satisfies the required closed-loop dynamics, and the synthesis of a control law that steers the trajectory of the system towards this surface. Within the proposed SMC control law, the sliding variable is associated with the tracking error and its derivatives as follows: [19]:

$$\sigma = \sigma(e, \dot{e}, ..., e^k) \tag{10}$$

The function $\sigma = 0$ defines a sliding surface (or manifold). The objective is to determine a control law that forces the system's trajectory to a region in which the sliding variable is equal to zero. This region is called the sliding surface (or manifold). The most commonly used choice for the sliding surface is a linear combination of the error and its derivatives:

$$\sigma = e^{(k)} + \sum_{i=0}^{k-1} c_i e^{(i)} \tag{11}$$

The parameter k is determined as *r-1*, where r represents the absolute difference of the highest degree of the output polynomial and the highest degree of the input polynomial. The typical form of the sliding plane is defined by the error and the parameter p:

$$\sigma = \left(\frac{d}{dt} + p\right)^k e \tag{12}$$

The choice of the parameter p is such that it creates a pole that reduces the dynamics of the system when moving along sliding surface. More precisely, k must be equal to $r-1$, with r being the relative degree between y and u. For $k = 1$ and $k = 2$ we have:

$$\begin{aligned} \sigma &= \dot{e} + pe, \quad k = 1 \\ \sigma &= \ddot{e} + 2p\dot{e} + p^2 e, \quad k = 2 \end{aligned} \tag{13}$$

It is crucial to choose the SMC control law so that the sliding surface exists and is reachable along system trajectories in finite time, so-called the reaching time.

After designing a sliding surface, the next step in SMC design is to derive a control law that guaranties that σ converges to zero in finite time. If a well-defined controller is able to drive the sliding variable σ to a neighborhood of zero, the sliding variable will consistently rise and fall around zero, resulting in a phenomenon called chattering. It causes an undesirable behavior of high-frequency control switching, resulting in a high-frequency vibration of the system [21]. Chattering can induce stress on the mechanical and electrical components of the structure, which can eventually destabilize the entire system [22]. In order to reduce the effects of chattering, continuous functions can be used to mimic the *sgn* function and replace its discontinuity.

In order to obtain a compromise between robustness to uncertainties and solve the chattering issue, we used the second-order SMC. It employs the "Super-Twisting" algorithm, with additional differentiators in the form of a multivariable controller. This algorithm is taken from [19] and is expressed by the following equations:

$$u = \lambda \sqrt{|\sigma|} sgn(\sigma) + w \tag{14}$$

$$\dot{w} = W \cdot sgn(\sigma) \tag{15}$$

$$\lambda = \sqrt{U} \qquad W = 1.1U \tag{16}$$

where U is a positive constant which is empirically determined, usually via simulation testing if the system's model is available. The parameter is calibrated using the trial and error process until the desired results are achieved. The control signal u manages the outputs of the system based on the output tracking error in the following manner:

$$\sigma = \sigma(e, \dot{e}) = e + \dot{e} \tag{17}$$

$$e(t) = r(t) - y(t) \tag{18}$$

where: $r(t)$ - reference input signal, $y(t)$ - output signal, and $e(t)$ - tracking error.

The super twisting-based controller is actually a nonlinear version of the PI controller, which can be graphically represented as in the Fig. 3. It is implemented using (14), (15) and (16).

The major benefit of the formulated control approach is the simplicity of its implementation, since only one parameter needs to be adjusted during the refinement phase. In order to illustrate the effectiveness and feasibility of the given control law, both simulation and experimental results are addressed.

IV. SIMULATION RESULTS

The nonlinear MIMO helicopter plant model as well as the STSMC are developed in the Matlab/Simulink environment. In order to determine the appropriate parameters of the STSMC controller, the simulations were repeated for their different values, and thus the obtained system responses were

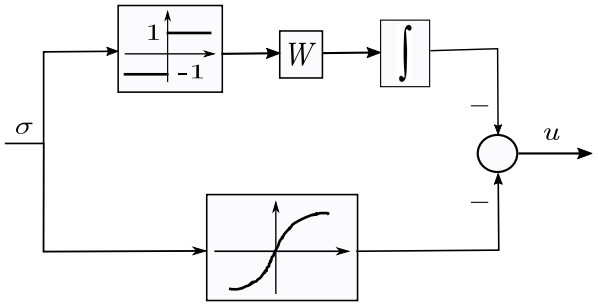

Fig. 3. Block scheme of STSMC controller

compared with the desired system output. In order to verify the efficiency of the STSMC controller, it is compared with PID and adaptive controllers. The used PID controller is described by the following equation:

$$u(t) = K_p e(t) + K_i \int_0^t u(\tau)d\tau + K_d \frac{de(t)}{dt} \tag{19}$$

where K_p, K_i and K_d are the coefficients for the proportional, integral, and derivative terms, respectively, $u(t)$ is control variable and $e(t)$ is error value between a desired setpoint and measured output process variable.

The parameters of the PID controller were determined experimentally, using the trial-error method [5]. Series of simulations are conducted with certain of its parameters until good results are obtained with the control system for azimuth and elevation angles. The adequate values of the PID controller parameters for elevation and azimuth angles obtained in this way are listed in the Table I.

TABLE I
PARAMETERS OF PID CONTROLLER

Angle	K_p	K_i	K_d
elevation	0.0157	0.003139	0.00872
azimuth	0.0523	0.000872	0.006978

An adaptive controller will be implemented as a PID controller with variable parameters (adaptive PID controller). It means that parameter values of the PID controller will be determined for several working points. To check the operation of the controller, randomly selected step signals of amplitudes that are in the working ranges of elevation and azimuth angle are used. The PID parameters tuning is performed using the Curve Fitting Tool in Matlab, where a function will be searched that would calculate the parameters depending on the current value of the angle. Functions are calculated for each of the parameters K_p, K_i and K_d for both elevation and azimuth angles. All functions are polynomial, some are of the fourth and some of the fifth order and are given by the expressions:

$$K_{p_e} = 3.69e^{-9}u^4 + 3.456e^{-7}u^3 + 6.938e^{-6}u^2 - 0.0002047u + 0.009773$$

$$K_{i_e} = -2.128e^{-11}u^5 - 3.016e^{-10}u^4 + 5.16e^{-8}u^3 + 2.417e^{-6}u^2 - 3.68e^{-5}u + 0.001851$$

$$K_{d_e} = 1.071e^{-9}u^4 + 1.598e^{-8}u^3 - 1.17e^{-6}u^2 - 6.158e^{-5}u + 0.004915$$

$$K_{p_a} = -3.363e^{-11}u^4 + 4.184e^{-10}u^3 + 4.46e^{-7}u^2 - 5.306e^{-6}u + 0.003763$$

$$K_{i_a} = 1.067e^{-11}u^4 - 2.069e^{-10}u^3 - 1.482e^{-7}u^2 - 3.74e^{-6}u + 0.004915$$

$$K_{d_a} = -4.001e^{-12}u^4 + 6.369e^{-10}u^3 + 6.182e^{-8}u^2 - 8.23e^{-6}u + 0.004113$$

Figs. 4 and 5 show the results obtained by the PID, adaptive and STSMC controllers for azimuth and elevation angles. In these graphs, the black line represents the reference signal, the blue line shows the output of the PID controlled system, the green line represents the output of adaptive controller and the output of the STSMC controlled system is shown by the red line. The control performance of employed controllers was evaluated with a complex reference signal consisting of a series of consecutive step excretions of different amplitude values. This form of input signal is chosen to simulate sudden changes that the helicopter might encounter in its operating environment.

It is obvious from the figures shown that the STSMC controller has no overshoot/undershoot and also reduces considerably the settling time and steady-state errors in comparison to the PID controller. A more significant deviation in settling time is observed with the PID controller, especially with azimuth control. The responses of both azimuth and elevation angles with the PID controller indicate their significant deviation from the reference signal within the duration of the first two-step signal. There are some minor overshoots and undershoots in the elevation angle response of the PID controller (Fig. 4), while the azimuth angle response with this controller is more oscillatory than with the STSMC (Fig. 5). The used adaptive controller exhibits slightly lower performance than SMC but significantly better than PID controllers. It is important to note that larger over/undershoots in the system responses can have catastrophic consequences for systems that need flight maneuvers such as take-off and landing [23]. Moreover, a system output that uses the STSMC controller satisfactorily tracked the reference signals without any significant delay.

In conclusion, the designed STSMC controller significantly outperforms the baseline PID controller in numerous quantities, most notably in its response time, rising time, and settlement time. In addition, the STSMC system's response has far less fluctuations than its PID counterpart, and remains steady throughout the observed time interval.

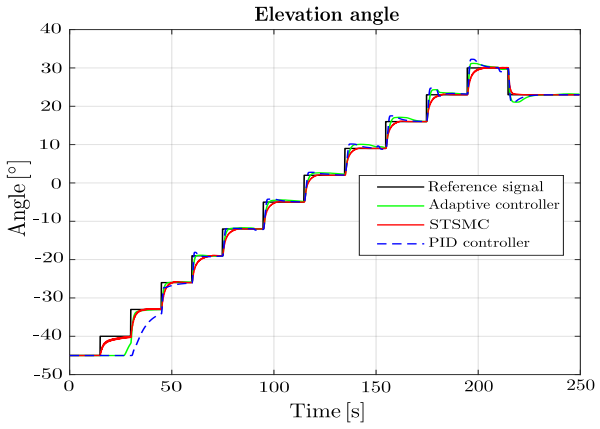

Fig. 4. Simulation results (elevation angle)

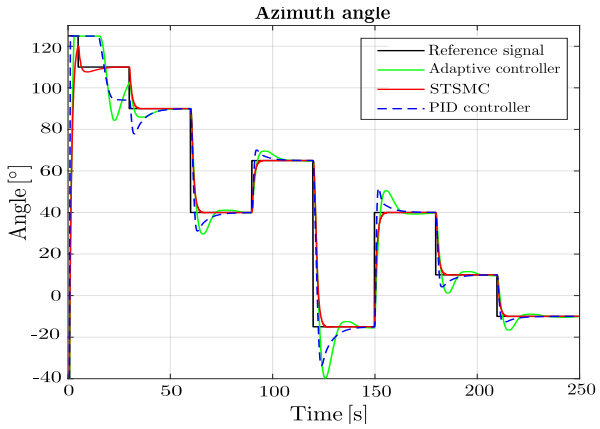

Fig. 5. Simulation results (azimuth angle)

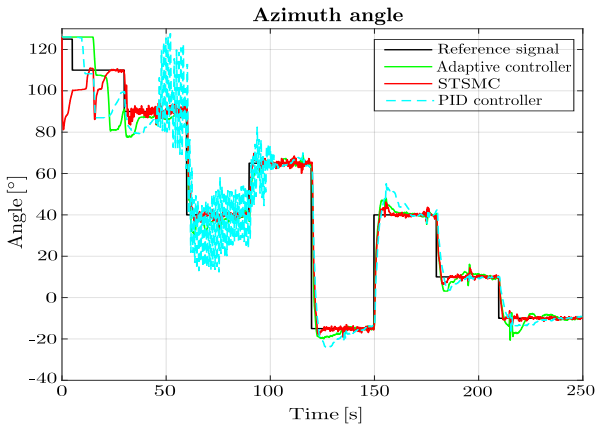

Fig. 6. Experimental results (azimuth angle)

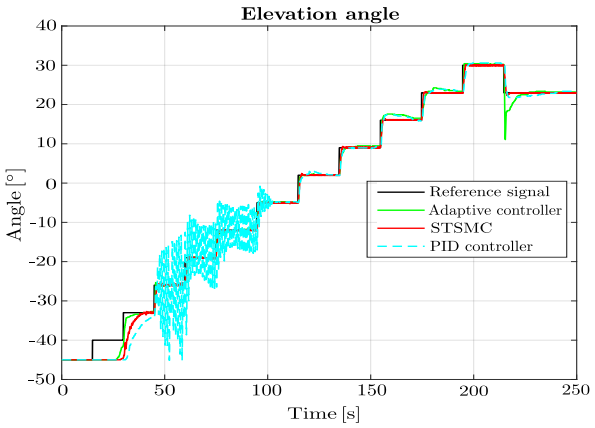

Fig. 7. Experimental results (elevation angle)

V. EXPERIMENTAL RESULTS

This section illustrates the experimental implementation of the STSMC control strategy on the Humusoft CE 150 physical helicopter system. In experimental evaluation of these controllers, the guidelines outlined in [24] were followed. The experiment involves integrating the developed controllers into a real system, comparing sensor outputs with reference values, and performing multiple execution sequences to ensure repeatability of the experiment under laboratory conditions.

In Figs. 6 and 7 the STSMC-based controller are compared to PID and adaptive controllers. These figures show the pitch angle and the yaw angle, respectively. Both plots illustrate a significant improvement of the STSMC controller compared to the PID controller. The azimuth and elevation angle time responses of the PID controller are more oscillatory than those of the STSMC controller, especially in the time interval between 50 and 110 seconds. On the contrary, the STSMC significantly reduces oscillations in azimuth and elevation angles, as well as a steady-state error trading overshoot for a faster response. Moreover, although there is an initial delay in following the reference values for both the elevation and azimuth angles, STSMC outperforms PID and adaptive controllers in this regard.

When analyzing the elevation and azimuth angle responses obtained using the adaptive controller, a significant improvement is observed compared to those obtained with PID controller. The oscillatory responses of both angles are significantly reduced with the adaptive controller. The reasons for this lie in the nature of adaptive regulators, since they are intended primarily for unstable systems. Therefore, this method is able to overcome the disturbances that occur due to coupling effects and achieve relatively good results. Oscillatory angle responses have larger amplitudes in the adaptive controller compared to the STSMC, but significantly smaller than in the PID controller. The STSMC is also characterized by faster tracking of the set value of the elevation angle, and minor oscillation when tracking the azimuth angle. It is important to emphasize that their amplitudes decreases with time.

A particular advantage of the STSMC is that it almost eliminated the coupling between the azimuth and elevation angles. Furthermore, the STSMC successfully copes with nonlinearities of the helicopter model and compensates the influence of the unmodeled dynamics of the helicopter model, which is difficult to achieve with the used PID-controller.

The time responses for the control signals for main and side motors for both PID and STSMC controllers are shown in Figs. 8 and 9. Control signals contain chattering which is related to the power consumption by helicopter model. In general, there is a trade-off between achieving good tracking performance and minimizing chattering in control input. It is important to note that attempting to reduce chattering in control signal increases the tracking error of the reference signal. Thus, it is crucial to designed such SMC control that simultaneously exhibited both the satisfactory tracking error and satisfactory chattering. It is evident that STSMC outperforms other considers controllers in terms of robustness properties and tracking performance with a satisfactory amplitude of chattering. On the other hand, with PID controllers, large amounts of oscillations of both angles with higher amplitude chattering in the control signals of both motors are noticeable in certain regions.

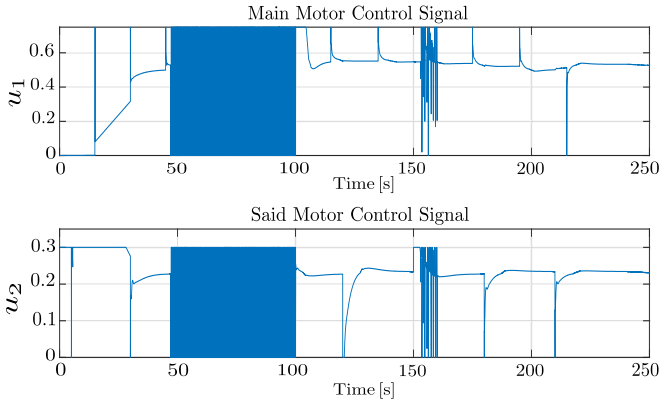

Fig. 8. Control signals u_1 and u_2 with PID control

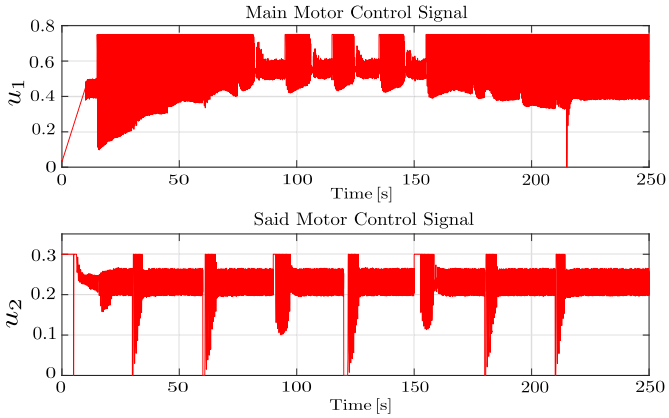

Fig. 9. Control signals u_1 and u_2 with STSMC control

VI. CONCLUSIONS

The super twisting sliding-mode-based control (STSMC) strategy for a nonlinear two-DOF helicopter model, as an inherently unstable system with strong coupling effects between the elevation and azimuth axes, was presented. Numerical simulations and experiments are provided to illustrate the capability of the STSMC control. The results obtained heavily imply that the STSMC approach significantly reduces the tracking error and oscillations in azimuth and elevation angles, and overall provides better control system performance than previously designed PID and adaptive controllers, despite modeling uncertainties as well as coupling between angles. The superiority of STSMC over PID and adaptive controllers is especially evident in the real-time implementation. Future work could focus on testing other robust control methods or different types of SMC control strategies with integration of adaptive control approaches.

ACKNOWLEDGMENT

This work has been supported in part by the scientific project "Strengthening Research and Innovation Excellence in Autonomous Aerial Systems - AeroSTREAM," supported by the European Commission HORIZON WIDERA-2021-ACCESS-05 Programme through the project under G.A. number 101071270.

REFERENCES

[1] Q. Zhu, Nonlinear systems: dynamics, control, optimization and applications to the science and engineering, Mathematics, vol.10, pp. 1-2, 2022.
[2] S. Vaidyanathan, C. Volos et al., Advances and Applications in Nonlinear Control Systems, Springer, 2016.
[3] J. Iqbal, M. Ullah, S. G. Khan, B. Khelifa, and S. Cukovic, Nonlinear control systems: brief overview of historical and recent advances, Nonlinear Engineering, vol. 6, pp. 301-312, 2017.
[4] U. Legat, R. Gajsek, and M. Gasperin, Simulation and control of a helicopter pilot plane, In Proc. 11th International Cultural and Academic Meeting of Engineering Students, 2005.
[5] J. Velagic, N. Osmic, E. Zunic, T. Uzunovic and A. Badnjevic, Design of 3d simulator for 2dof helicopter model control, In Proc. ELMAR, 2010, pp. 305-308.
[6] N. Shen, Z. Su, X. Wang, and Y. Li, Robust controller design and hardware-in-loop simulation for a helicopter, In Proc. 4th IEEE Conf. on Indust. Electronics and Applications, 2009, pp. 3187-3191.
[7] E. Dragolj, J. Velagic and N. Osmic, Modelling of nonlinear helicopter model and loopshaping based controller synthesis, In Proc. 39th Conference of IEEE Indust. Electronics Society, 2013, pp. 3603-3608.
[8] M. Smid et al., Prediktivni rizeni modelu helikoptery, 2021.
[9] A. Salihbegovic, Multivariable sliding mode approach with enhanced robustness properties based on the robust internal-loop compensator for a class of nonlinear mechanical systems, In Proc. European Control Conference (ECC), IEEE, 2016, pp. 382-387.
[10] M. R. Kafi, H. Chaoui, S. Miah and A. Debilou, Local model networks based mixed-sensitivity h-infinity control of ce-150 helicopters, Control Theory and Technology, vol. 15, pp. 34-44, 2017.
[11] J. Velagic and N. Osmic, Fuzzy-genetic identification and control stuctures for nonlinear helicopter model, Intelligent Automation and Soft Computing, vol. 19, pp. 51-68, 2013.
[12] M. H. Younis and R. Quraishi, Adaptive fuzzy control for twin rotor helicopter stabilization, In Proc. 2nd International Conference on Latest trends in Electrical Engineering and Computing Technologies, 2019, pp. 1-5.
[13] J. A. Vilchis, B. Brogliato, A. Dzul and R. Lozano, Nonlinear modelling and control of helicopters, Automatica, vol. 39, pp. 1583-1596, 2003.
[14] T. Uzunovic, J. Velagic, N. Osmic, A. Badnjevic and E. Zunic, Neural networks for helicopter azimuth and elevation angles control obtained by cloning processes, In Proc. IEEE International Conference on Systems, Man and Cybernetics, 2010, pp. 1076-1082.
[15] Humusoft, CE 150 Helicopter Model, User's Manual, Prague, 2007.
[16] P. Horacek, CE 150 HELICOPTER MODEL, Educational manual, Humosoft Ltd., Czech Republic, 2007.
[17] N. Osmic, J. Velagic, S. Konjicija and A. Galijasevic, Genetic algorithm based identification of a nonlinear 2dof helicopter model, In Proc. 18th Mediterranean Conference on Control and Automation, 2010, pp. 333-338.
[18] S. Li, X. Yu, L. Fridman, Z. Man and X. Wang, Advances in Variable Structure Systems and Sliding Mode Control-Theory and Applications, Springer, 2017.
[19] R. DeCarlo and S. Zak, A quick introduction to sliding mode control and its applications, Universita Degli Studi di Cagliari, 2008.
[20] M. Harvey, A comparative study of sliding mode control algorithms implemented on a 2-DOF planar robot, University of Alabama, 2015.
[21] A. Levant, Chattering analysis, IEEE Transactions on Automatic Control, vol. 55, pp. 1380-1389, 2010.
[22] K. D. Young, V. I. Utkin and U. Ozguner, A control engineer's guide to sliding mode control, IEEE Transactions on Control Systems Technology, vol. 7, pp. 328-342, 1999.
[23] G. Zhao, D. Nesic, Y. Tan and C. Hua, Overcoming overshoot performance limitations of linear systems with reset control, Automatica, vol. 101, pp. 27-35, 2019.
[24] F. Shull, J. Singer and D. I. Sjoberg, Guide to advanced empirical software engineering, Springer, 2008, vol. 93.